Output-Feedback Cooperative Formation Maneuvering of Autonomous Surface Vehicles With Connectivity Preservation and Collision Avoidance

Zhouhua Peng, *Member, IEEE*, Dan Wang, *Senior Member, IEEE*, Tieshan Li, *Senior Member, IEEE*, and Min Han, *Senior Member, IEEE*

***Abstract*—In this paper, a cooperative time-varying formation maneuvering problem with connectivity preservation and collision avoidance is investigated for a fleet of autonomous surface vehicles (ASVs) with position–heading measurements. Each vehicle is subject to unknown kinetics induced by internal model uncertainty and external disturbances. At first, a nonlinear state observer is used to recover the unmeasured linear velocity and yaw rate as well as unknown uncertainty and disturbances. Then, observer-based cooperative time-varying formation maneuvering control laws are designed based on artificial potential functions, nonlinear tracking differentiators, and a backstepping technique. The stability of closed-loop distributed formation control system is analyzed based on input-to-state stability and cascade stability. The salient features of the proposed method are as follows. First, cooperative time-varying formation maneuvering with the capability of connectivity preservation and collision avoidance can be achieved in the absence of velocity measurements. Second, the complexity of the cooperative time-varying formation maneuvering control laws is reduced without resorting to dynamic surface control. Third, the uncertainty and disturbance are actively rejected in the presence of position–heading measurements. Simulation results are given to substantiate the proposed output feedback control method for cooperative time-varying formation maneuvering of ASVs with connectivity preservation and collision avoidance.**

***Index Terms*—Autonomous surface vehicles (ASVs), collision avoidance, connectivity preservation, state observer, time-varying formation maneuvering.**

I. Introduction

FORMATION control of multiple marine vehicles has drawn compelling interest from various communities due to its wide applications in ocean engineering fields, such as sensor networks, coordinated search and rescue, marine survey, etc. [1]–[11]. Marine operations by utilizing a fleet of marine vehicles contribute to improved efficiency and effectiveness over a single vehicle. In the literature, various formation control schemes are proposed, including leader–follower approach [12]–[14], virtual structure, graph-based mechanism [15]–[19], etc. In particular, graph-based distributed formation control methods have been widely explored for surface vehicles [16]–[18], [20], [21], and the key advantage is that a collective formation pattern can be reached though local information exchanges [22]–[29]. However, the restriction of the results in [16]–[18], [20], and [21] is twofold. First, the collision avoidance among vehicles is not considered [16]–[18], [20], [21]. Second, the network is not assured to be connected in the presence of limited communication range in a sea environment.

Surface vehicles moving at a complex sea environment inevitably come across various static and dynamic obstacles, and collisions may occur when achieving a collective formation [30]. Therefore, collision avoidance capability is of critical importance for safe maneuvering of multiple marine vehicles [31]–[33]. Prevailing collision avoidance approaches include behavior-based method, potential functions [15], and prescribed performance technique [31]–[33]. In addition to collision avoidance, connectivity is desired to be connected during the coordination of multivehicle systems [34]–[38]. It is worthwhile mentioning that all aforementioned results [15], [31]–[33] assume that full state information is available for feedback design. However, the position and heading of marine vehicles can be obtained by using GPS device and magnetic compass, while their velocities may not be easily obtained. From a practical perspective, it is

Manuscript received October 25, 2018; revised March 10, 2019; accepted April 30, 2019. Date of publication June 5, 2019; date of current version May 7, 2020. This work was supported in part by the National Natural Science Foundation of China under Grant 51579023, Grant 61673081, and Grant 61773087, in part by the Innovative Talents in Universities of Liaoning Province under Grant LR2017014, in part by the High-Level Talent Innovation and Entrepreneurship Program of Dalian under Grant 2016RQ036, in part by the Training Program for High-Level Technical Talent in Transportation Field under Grant 2018-030, in part by the National Key Research and Development Program of China under Grant 2016YFC0301500, in part by the Fundamental Research Funds for the Central Universities under Grant 3132019013, in part by the Fundamental Research Program for Key Laboratory of the Education Department of Liaoning Province under Grant LZ2015006, and in part by the Science and Technology Innovation Funds of Dalian under Grant 2018J11CY022. This paper was recommended by Associate Editor Y. Shi. *(Corresponding authors: Zhouhua Peng; Dan Wang.)*

Z. Peng and D. Wang are with the School of Marine Electrical Engineering, Dalian Maritime University, Dalian 116026, China, and also with the Collaborative Innovation Institute of Unmanned Ships, Dalian Maritime University, Dalian 116026, China (e-mail: zhpeng@dlmu.edu.cn; dwangdl@gmail.com).

T. Li is with the Navigation College, Dalian Maritime University, Dalian 116026, China (e-mail: tieshanli@126.com).

M. Han is with the Electronic Information and Electrical Engineering Department, Dalian University of Technology, Dalian 116024, China (e-mail: minhan@dlut.edu.cn).

Color versions of one or more of the figures in this paper are available online at http://ieeexplore.ieee.org.

Digital Object Identifier 10.1109/TCYB.2019.2914717

rewarding to investigate the distributed time-varying formation maneuvering control of surface vehicles based on output information [39]–[43].

Motivated by the above observations, this paper addresses the output feedback control for cooperative time-varying formation maneuvering of autonomous surface vehicles (ASVs) subject to unmeasured velocities and unknown kinetics. A practical design method is presented for developing the distributed time-varying formation maneuvering control laws with the capability of avoiding obstacles and collisions between neighboring vehicles, in addition to preserving connectivity. Specifically, a nonlinear state observer is used to recover the unmeasured velocity and yaw rate of each ASV as well as unknown uncertainty and disturbances. Then, distributed output feedback formation maneuvering control laws are designed with the aid of nonlinear state observers, artificial potential functions, nonlinear tracking differentiators, and a backstepping technique. Finally, the stability of closed-loop distributed formation maneuvering system is analyzed based on input-to-state stability and cascade stability. Simulation results are provided to substantiate the proposed output feedback for cooperative time-varying formation maneuvering of ASVs while avoiding collisions and preserving connectivity.

Compared with the existing results, the salient features of the proposed design method for cooperative time-varying formation maneuvering of ASVs are as follows. First, in contrast to the state feedback formation control laws proposed in [13], [31]–[33], and [44] the output feedback formation maneuvering control laws without using velocity measurements are proposed herein. Second, compared with the works [13], [31]–[33], where dynamic surface control is used to reduce the complexity of formation control laws, the proposed control laws are simplified without using the dynamic surface control. Third, the vehicle uncertainties are estimated based on velocity measurements [13], [16], [18], [31]–[33], while both vehicle velocities and vehicle uncertainties can be estimated by using position–yaw measurements. Moreover, only one parameter is required to be tuned in the observer and the complexity of distributed time-varying formation control laws is reduced drastically compared with the approximation-based control.

The remainder of this paper is organized as follows. Section II introduces some preliminaries and states the problem formulation. Section III gives the observer-based distributed formation maneuvering controller design. Section IV provides the cascade stability analysis. Section V gives an example for illustrations. Section VI concludes this paper.

Throughout this paper, $||\cdot||$ denotes the 2-norm of a vector. $\lambda_{\min}(\cdot)$ and $\lambda_{\max}(\cdot)$ denote the minimum and maximum of a symmetric matrix.

II. Preliminaries and Problem Formulation

A. Collision Avoidance

In order to assure collision-free cooperative time-varying formation maneuvering between ASVs, the following potential functions are introduced [45]:

$$V_{ij}^{c}(p_{ij}) = \begin{cases} \left(\dfrac{\bar{R}^2-\|p_{ij}\|^2}{\|p_{ij}\|^2-\underline{R}^2}\right)^2, & \underline{R} \le \|p_{ij}\| \le \bar{R} \\ 0, & \|p_{ij}\| > \bar{R} \text{ or } \|p_{ij}\| < \underline{R} \end{cases} \tag{1}$$

and its partial derivative with respect to p_i is given by

$$\frac{\partial V_{ij}^{c}}{\partial p_i} = \begin{cases} \dfrac{4(\bar{R}^2-\underline{R}^2)\left(\|p_{ij}\|^2-\bar{R}^2\right)}{\left(\|p_{ij}\|^2-\underline{R}^2\right)^3} p_{ij}, & \underline{R} < \|p_{ij}\| < \bar{R} \\ 0_2, & \|p_{ij}\| \ge \bar{R} \text{ or } \|p_{ij}\| < \underline{R} \end{cases} \tag{2}$$

where $p_{ij} = p_i - p_j$ and $p_i = [x_i, y_i]^T$; $\underline{R}$ is the smallest safe collision avoidance radius; and $\bar{R}$ is the detection range. Note that both V_{ij}^{c} and $\partial V_{ij}^{c}/\partial p_i$ are continuous at $\|p_{ij}\| = \bar{R}$. Hence, V_{ij}^{c} is continuously differential with respect to the domain $\|p_{ij}\| > \bar{R}$. Besides, V_{ij}^{c} monotonically decreases when $\|p_{ij}\| > \underline{R}$, and $\partial V_{ij}^{c}/\partial p_i = -\partial V_{ij}^{c}/\partial p_j = \partial V_{ji}^{c}/\partial p_i = -\partial V_{ji}^{c}/\partial p_j$.

B. Obstacle Avoidance

In order to avoid collisions with static obstacles in complex ocean environment, the following potential functions are introduced [45]:

$$V_{ik}^{o}(p_{ik}) = \begin{cases} \left(\dfrac{\bar{R}_o^2-\|p_{ik}\|^2}{\|p_{ik}\|^2-\underline{R}_o^2}\right)^2, & \underline{R}_o \le \|p_{ik}\| \le \bar{R}_o \\ 0, & \|p_{ik}\| > \bar{R}_o \text{ or } \|p_{ik}\| < \underline{R}_o \end{cases} \tag{3}$$

and its partial derivative with respect to p_i is given by

$$\frac{\partial V_{ik}^{o}}{\partial p_i} = \begin{cases} \dfrac{4(\bar{R}_o^2-\underline{R}_o^2)(\|p_{ik}\|^2-\bar{R}_o^2)p_{ik}}{\left(\|p_{ik}\|^2-\underline{R}_o^2\right)^3}, & \underline{R}_o < \|p_{ik}\| < \bar{R}_o \\ 0_2, & \|p_{ik}\| \ge \bar{R}_o \text{ or } \|p_{ik}\| < \underline{R}_o \end{cases} \tag{4}$$

where $p_{ik} = p_i - p_k$; $0_2 = [0, 0]^T$; $\underline{R}_o$ is the smallest safe collision avoidance radius with respect to the obstacle; and $\bar{R}_o$ is the detection range. Hence, V_{ik}^{o} is continuously differential with respect to the domain $\|p_{ik}\| > \bar{R}$. Besides, V_{ik}^{o} monotonically decreases when $\|p_{ik}\| > \underline{R}$, and $\partial V_{ik}^{o}/\partial p_i = \partial V_{ki}^{o}/\partial p_i$, $\partial V_{ik}^{o}/\partial p_k = \partial V_{ki}^{o}/\partial p_k = 0$. The distances between two obstacles are assumed to be larger than $2\bar{R}_o$.

C. Connectivity Preservation

Connectivity maintenance functions are used to keep connectivity of ASV pairs which are inside the preservation regions and are chosen as

$$V_{ij}^{m}(p_{ij}) = \begin{cases} \dfrac{1}{2\left(\bar{R}_m^2-\|p_{ij}\|^2\right)}, & \underline{R}_m < \|p_{ij}\| < \bar{R}_m \\ 0, & \|p_{ij}\| \ge \bar{R}_m \text{ or } \|p_{ij}\| \le \underline{R}_m \end{cases} \tag{5}$$

and its partial derivative with respect to p_{ij} is given by

$$\frac{\partial V_{ij}^{m}}{\partial p_i} = \begin{cases} \dfrac{p_{ij}}{\left(\bar{R}_m^2-\|p_{ij}\|^2\right)^2}, & \underline{R}_m < \|p_{ij}\| < \bar{R}_m \\ 0_2, & \|p_{ij}\| \ge \bar{R}_m \text{ or } \|p_{ij}\| \le \underline{R}_m \end{cases} \tag{6}$$

where $\bar{R}_m$ is the maximal communication range and $\underline{R}_m$ is the minimal range when the connectivity maintenance function is active.

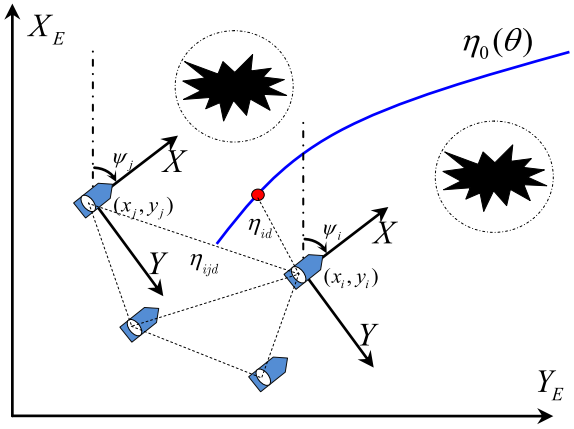

Fig. 1. Reference frames.

D. Problem Formulation

Consider a fleet of ASVs with the ith vehicle dynamics described as [46]

$$\dot{\eta}_i = R_i(\psi_i)v_i, \quad i = 1, \ldots, N \tag{7}$$

$$M_i\dot{v}_i + C_i(v_i)v_i + D_i(v_i)v_i + g_i(v_i, \eta_i) = w_i + \tau_i \tag{8}$$

where $\eta_i = [x_i, y_i, \psi_i]^T \in \Re^3$ denotes the position and heading. $R_i(\psi_i) \in \Re^{3\times 3}$ is a rotate matrix given by

$$R_i(\psi_i) = \begin{bmatrix} \cos(\psi_i) & -\sin(\psi_i) & 0 \\ \sin(\psi_i) & \cos(\psi_i) & 0 \\ 0 & 0 & 1 \end{bmatrix}. \tag{9}$$

$v_i = [u_i, v_i, r_i]^T \in \Re^3$ are the surge, sway, and yaw velocities in the body-fixed reference frame as shown in Fig. 1. $M_i^T = M_i \in \Re^{3\times 3}$ is the inertial matrix. $D_i(v_i) \in \Re^{3\times 3}$ is a nonlinear damping matrix. $C_i(v_i) = -C_i(v_i)^T \in \Re^{3\times 3}$ denotes a Coriolis and centripetal matrix. $\tau_i = [\tau_{1i}, \tau_{2i}, \tau_{3i}]^T \in \Re^3$ is a control input. $w_i = [w_{1i}, w_{2i}, w_{3i}]^T \in \Re^3$ denotes the vector of unknown disturbances induced by the wind, waves, and ocean currents. $g_i(v_i, \eta_i) \in \Re^3$ represents the unmodeled hydrodynamics.

The ASV group is guided by a virtual leader moving along a path parameterized by

$$\eta_0(\theta) = \left[x_0(\theta), y_0(\theta), \psi_0(\theta)\right]^T$$
$$\psi_0(\theta) = \arctan\left(y_0^\theta(\theta)/x_0^\theta(\theta)\right) \tag{10}$$

where $(\cdot)^\theta(\theta) = \partial(\cdot)(\theta)/\partial\theta \in \Re^3$ is the partial derivative of $(\cdot)(\theta) \in \Re^3$; $\theta \in \Re$ is a path variable. It is assumed that $\eta_0^\theta(\theta)$ is bounded.

Let $\mathcal{V} = \{n_0, n_1, \ldots, n_N\}$ be a node set and $\mathcal{E} = \{(i, j) \in \mathcal{V} \times \mathcal{V}\}$ be an edge set. The communication graph among the ASVs and the leader can be described by a graph $\mathcal{G} = \{\mathcal{V}, \mathcal{E}\}$. The following assumption is made on the graph $\mathcal{G}$.

Assumption 1: The graph $\mathcal{G}$ contains a spanning tree with the root node being the node n_0.

Problem 1: The cooperative time-varying formation maneuvering of ASVs with collision avoidance, obstacle avoidance, and connectivity preservation is to achieve the following objectives.

1) *Geometric Objective:* The ASVs are driven to achieve a time-varying formation pattern with relative position and orientation as follows:
$$\lim_{t\to\infty} \|\eta_i(t) - \eta_{id} - \eta_0(\theta(t))\| < l_1 \tag{11}$$
where $l_1 \in \Re$ is a small positive constant. $\eta_{id} \in \Re^3$ denotes the desired formation position and orientation with respect to the virtual leader.
2) *Dynamic Objective:* The derivative of the path variable θ converges to a desired speed $u_s(t)$ as
$$\lim_{t\to\infty} \left\|\dot{\theta}(t) - u_s(t)\right\| < l_2 \tag{12}$$
where $l_2 \in \Re$ is a small positive constant.
3) *Collision and Obstacle Avoidance:* The collisions among vehicles and obstacles can be avoided such that
$$\left\|p_i(t) - p_j(t)\right\| > \underline{R}, \|p_i(t) - p_k(t)\| > \underline{R}_o \tag{13}$$
where $\underline{R} \in \Re$ and $\underline{R}_o \in \Re$ are the smallest collision avoidance radii.
4) *Connectivity Preservation:* The network is connected such that
$$\left\|p_i(t) - p_j(t)\right\| < \bar{R}_m \tag{14}$$
provided that the agents are initially connected, that is, $\|p_i(0) - p_j(0)\| < \bar{R}_m$. $\bar{R}_m$ is the maximal communication range.

III. Observer-Based Distributed Time-Varying Formation Maneuvering

A. Observer

In this section, a nonlinear state observer is used for estimating the system uncertainties as well as recovering the unmeasured surge, sway, and yaw rate information using the obtained position–heading information. To this end, the ASV dynamics (7), (8) is rewritten in a compact form as

$$\begin{cases} \dot{\eta}_i = R_i(\psi_i)v_i \\ \dot{v}_i = \zeta_i + M_i^{-1}\tau_i \end{cases} \tag{15}$$

where $\zeta_i = [\zeta_{ui}, \zeta_{vi}, \zeta_{ri}]^T \in \Re^3$ is a state vector expressed as $\zeta_i = M_i^{-1}[-C_i(v_i)v_i - D_i(v_i)v_i - g_i(v_i, \eta_i) + w_i(t)]$.

The following assumption is made during the nonlinear observer design.

Assumption 2: There exists a positive constant ζ_i^* such that $\|\dot{\zeta}_i\| \le \zeta_i^*$.

ζ_i is a vector of velocity-related functions, and it is natural to assume that their derivatives are bounded. Besides, because the energy of external disturbances and control inputs to drive ASVs is limited, Assumption 2 is reasonable.

A full-order state observer is used for estimating the unmeasured velocity and unknown uncertainty as follows:

$$\begin{cases} \dot{\hat{\eta}}_i = -K_{1i}^o\left(\hat{\eta}_i - \eta_i\right) + R_i(\psi_i)\hat{v}_i \\ \dot{\hat{v}}_i = -K_{2i}^o R_i^T(\psi_i)\left(\hat{\eta}_i - \eta_i\right) + \hat{\zeta}_i + M_i^{-1}\tau_i \\ \dot{\hat{\zeta}}_i = -K_{3i}^o R_i^T(\psi_i)\left(\hat{\eta}_i - \eta_i\right) \end{cases} \tag{16}$$

where $\hat{\eta}_i = [\hat{x}_i, \hat{y}_i, \hat{\psi}_i]^T \in \Re^3$, $\hat{v}_i = [\hat{u}_i, \hat{v}_i, \hat{r}_i]^T \in \Re^3$, $\hat{\zeta}_i = [\hat{\zeta}_{ui}, \hat{\zeta}_{vi}, \hat{\zeta}_{ri}]^T \in \Re^3$ and $\hat{x}_i$, $\hat{y}_i$, $\hat{\psi}_i$, $\hat{u}_i$, $\hat{v}_i$, $\hat{r}_i$, $\hat{\zeta}_{ui}$, $\hat{\zeta}_{vi}$, and $\hat{\zeta}_{ri}$ are the estimates of x_i, y_i, ψ_i, u_i, v_i, r_i, ζ_{ui}, ζ_{vi}, and ζ_{ri},

respectively. $K_{1i}^o \in \Re^{3\times3}$, $K_{2i}^o \in \Re^{3\times3}$, and $K_{3i}^o \in \Re^{3\times3}$ are observer matrices and they are selected as $[K_{1i}^o, K_{2i}^o, K_{3i}^o]^T = [3\omega_i I_3, 3\omega_i^2 I_3, \omega_i^3 I_3]^T$, where ω_i is the observer bandwidth. Only one parameter ω_i is required in the observer, and the tuning process can be much simpler than the existing neural-network-based observer [17]. The inertial matrix M_i can be determined by mechanism modeling or identification process. As a result, a nominal inertial matrix can be used in implementation.

The error dynamics of the observer from (15) and (16) can be expressed as

$$\begin{cases} \dot{\tilde{\eta}}_i = -K_{1i}^o \tilde{\eta}_i + R_i(\psi_i)\tilde{\nu}_i \\ \dot{\tilde{\nu}}_i = -K_{2i}^o R_i^T(\psi_i)\tilde{\eta}_i + \tilde{\zeta}_i \\ \dot{\tilde{\zeta}}_i = -K_{3i}^o R_i^T(\psi_i)\tilde{\eta}_i - \dot{\zeta}_i \end{cases} \tag{17}$$

where $\tilde{\eta}_i = \hat{\eta}_i - \eta_i$, $\tilde{\nu}_i = \hat{\nu}_i - \nu_i$, and $\tilde{\zeta}_i = \hat{\zeta}_i - \zeta_i$ are estimation errors. In what follows, the error dynamics (17) can be put into a matrix form as

$$\dot{\tilde{X}}_i = A_i \tilde{X}_i - B_i \dot{\zeta}_i \tag{18}$$

where $\tilde{X}_i = [\tilde{\eta}_i^T, \tilde{\nu}_i^T, \tilde{\zeta}_i^T]^T \in \Re^9$ and

$$A_i = \begin{bmatrix} -K_{1i}^o & R_i(\psi_i) & 0_{3\times3} \\ -K_{2i}^o R_i^T(\psi_i) & 0_{3\times3} & I_3 \\ -K_{3i}^o R_i^T(\psi_i) & 0_{3\times3} & 0_{3\times3} \end{bmatrix}, \ B_i = \begin{bmatrix} 0_{3\times3} \\ 0_{3\times3} \\ I_3 \end{bmatrix}. \tag{19}$$

By introducing a state transformation $E_{io} = T_i \tilde{X}_i$ with $T_i = \text{diag}\{R_i^T(\psi_i), I_3, I_3\}$, (18) becomes

$$\dot{E}_i = A_{0i} E_{io} + r_i S_{Ti} E_{io} - B_i \dot{\zeta}_i \tag{20}$$

where

$$A_{0i} = \begin{bmatrix} -K_{1i}^o & I_{3\times3} & 0_{3\times3} \\ -K_{2i}^o & 0_{3\times3} & I_3 \\ -K_{3i}^o & 0_{3\times3} & 0_{3\times3} \end{bmatrix}, \ S = \begin{bmatrix} 0 & -1 & 0 \\ 1 & 0 & 0 \\ 0 & 0 & 0 \end{bmatrix} \tag{21}$$

and $S_{Ti} = \text{diag}\{S^T, 0_{3\times3}, 0_{3\times3}\}$.

Remark 1: The observer in (16) relies on the absolute position information of the vehicle. When the absolute position information is not available, it is desirable to design an observer based on relative information.

B. Controller

At first, a cooperative formation maneuvering error based on the information of neighbors is defined as

$$z_{1i} = R_i^T \Big[\sum_{j=1}^N a_{ij}\big(\eta_i - \eta_j - \eta_{ijd}\big) + a_{i0}(\eta_i - \eta_0(\theta) - \eta_{id}) \Big] \tag{22}$$

where $R_i = R_i(\psi_i)$, $\eta_{ijd} = \eta_{id} - \eta_{jd} \in \Re^3$. In case that the ith ASV obtain the path information, $a_{i0} = 1$; otherwise, $a_{i0} = 0$. Similarly, if the ith vehicle obtain the position and heading information of the jth ASV, $a_{ij} = 1$; otherwise, $a_{ij} = 0$.

By differentiating z_{1i} and using (7) and (8), it leads to

$$\begin{cases} \dot{z}_{1i} = -r_i S z_{1i} + a_{si}\nu_i - \sum_{j=1}^N a_{ij} R_i^T R_j \nu_j \\ \qquad - a_{i0} R_i^T \eta_0^\theta(\theta)\dot{\theta} - \sum_{j=0}^N a_{ij} R_i^T \dot{\eta}_{ijd} \\ \dot{\nu}_i = \zeta_i + M_i^{-1}\tau_i \end{cases} \tag{23}$$

where $a_{si} = \sum_{j=0}^N a_{ij}$ and $R_j = R_j(\psi_j)$.

Letting $u_s - \vartheta = \dot{\theta}$, it follows that:

$$\begin{cases} \dot{z}_{1i} = -r_i S z_{1i} + a_{si}\nu_i - \sum_{j=1}^N a_{ij} R_i^T R_j \nu_j \\ \qquad - a_{i0} R_i^T \eta_0^\theta(\theta)(u_s - \vartheta) - \sum_{j=0}^N a_{ij} R_i^T \dot{\eta}_{ijd} \\ \dot{\nu}_i = \zeta_i + M_i^{-1}\tau_i. \end{cases} \tag{24}$$

Step 1: To achieve the cooperative time-varying formation control with the capability of collision avoidance and connectivity preservation, a kinematic control law ν_i^c is proposed as follows:

$$\nu_i^c = \Bigg(-\frac{K_{1i} q_i}{\sqrt{\|q_i\|^2 + \Delta_{1i}^2}} + \sum_{j=1}^N a_{ij} R_i^T R_j \hat{\nu}_j + a_{i0} R_i^T \eta_0^\theta(\theta) u_s + \sum_{j=0}^N a_{ij} R_i^T \dot{\eta}_{ijd} \Bigg) \Big/ a_{si} \tag{25}$$

where $q_i = z_{1i} + R_i^T z_{3i}$ with

$$z_{3i} = \sum_{j=1}^N \frac{\partial V_{ij}^c}{\partial \eta_i} + 2\sum_{k=1}^{N_o} \frac{\partial V_{ik}^o}{\partial \eta_i} + \sum_{j=1}^N \frac{\partial V_{ij}^m}{\partial \eta_i} \tag{26}$$

$K_{1i} \in \Re^{3\times3}$ is a diagonal matrix; $\Delta_{1i} \in \Re$ is a positive constant. The introduction of Δ_{1i} helps to avoid large virtual control signal during transient.

In order to update θ smoothly, a filtering scheme is used to update ϑ as follows:

$$\dot{\vartheta} = -\lambda\Big(\vartheta + \mu \sum_{i=1}^N a_{i0}\big(\eta_0^\theta(\theta)\big)^T R_i q_i\Big) \tag{27}$$

where $\lambda \in \Re$ and $\mu \in \Re$ are positive constants. For details, the readers are referred to [46].

Substituting (27) into (25) and using (16), it follows that:

$$\begin{cases} \dot{z}_{1i} = -r_i S z_{1i} - \frac{K_{1i} q_i}{\sqrt{\|q_i\|^2 + \Delta_{1i}^2}} + a_{si}(-\tilde{\nu}_i + z_{2i}) \\ \qquad + a_{i0} R_i^T \eta_0^\theta(\theta)\vartheta + \sum_{j=1}^N a_{ij} R_i^T R_j \tilde{\nu}_j \\ \dot{z}_{2i} = -K_{2i}^o R_i^T \tilde{\eta}_i + \hat{\zeta}_i + M_i^{-1}\tau_i - \nu_{id}^c - a_{si} q_i \end{cases} \tag{28}$$

where $z_{2i} = \hat{\nu}_i - \nu_i^c$ and $\nu_{id}^c = \dot{\nu}_i^c$.

Step 2: In order to stabilize z_{2i}, an anti-disturbance kinetic controller is proposed as follows:

$$\tau_i = M_i \left(-\frac{K_{2i} z_{2i}}{\sqrt{\|z_{2i}\|^2 + \Delta_{2i}^2}} - a_{si} q_i - \hat{\zeta}_i + \hat{\nu}_{id}^c \right) \tag{29}$$

where $K_{2i} \in \Re^{3\times3}$ is a diagonal matrix and $\Delta_{2i} \in \Re$ is a positive constant. $\hat{\nu}_{id}^c$ is an estimate of $\dot{\nu}_i^c$ and will be designed in step 3. The introduction of the TD is to reduce the calculation complexity of the cooperative time-varying formation maneuvering control laws.

Substituting (29) into (28), it leads to

$$\begin{cases} \dot{z}_{1i} = -r_i S z_{1i} - \frac{K_{1i} q_i}{\sqrt{\|q_i\|^2 + \Delta_{1i}^2}} + a_{si}(-\tilde{\nu}_i + z_{2i}) \\ \qquad + a_{i0} R_i^T \eta_0^\theta(\theta)\vartheta + \sum_{j=1}^N a_{ij} R_i^T R_j \tilde{\nu}_j \\ \dot{z}_{2i} = -\frac{K_{2i} z_{2i}}{\sqrt{\|z_{2i}\|^2 + \Delta_{2i}^2}} - a_{si} q_i + \tilde{\nu}_{id}^c \\ \qquad - K_{2i}^o R_i^T \tilde{\eta}_i \end{cases} \tag{30}$$

where $\tilde{\nu}_{id}^c = \hat{\nu}_{id}^c - \nu_{id}^c$.

Step 3: Let ν_i^c pass through a finite-time nonlinear TD to obtain an accurate estimate of $\dot{\nu}_i^c$ as follows [47]:

$$\begin{cases} \dot{\hat{\nu}}_i^c = \hat{\nu}_{id}^c \\ \dot{\hat{\nu}}_{id}^c = -\gamma_i^2 \left\{ k_{i1} \left[\hat{\nu}_i^c - \nu_i^c \right]^{\rho_{i1}} + k_{i2} \left[\frac{\hat{\nu}_{id}^c}{\gamma_i} \right]^{\rho_{i2}} \right\} \end{cases} \tag{31}$$

where $\hat{\nu}_i^c \in \mathbb{R}^3$ and $\hat{\nu}_{id}^c \in \mathbb{R}^3$ are the estimates of ν_i^c and $\dot{\nu}_i^c$. $k_{i1} \in \mathbb{R}^{3\times 3}$, $k_{i2} \in \mathbb{R}^{3\times 3}$, $\rho_{i1} \in \mathbb{R}$, and $\rho_{i2} \in \mathbb{R}$ are design parameters. $[b]^\rho = [\text{sign}(b_1)|b_1|^\rho, \ldots, \text{sign}(b_N)|b_N|^\rho]^T$, where $b = [b_1, \ldots, b_N]^T$ and ρ is a positive constant. According to [47], there exist positive constants l_i^* and l_{id}^* such that

$$\left\| \hat{\nu}_i^c - \nu_i^c \right\| \le l_i^*, \left\| \hat{\nu}_{id}^c - \nu_{id}^c \right\| \le l_{id}^*. \tag{32}$$

Note that $\hat{\nu}_{id}^c$ is continuous due to the integration, which make the control signal τ_i free from chattering.

Remark 2: The control law design procedure follows the backstepping design technique with the exception that a finite-time nonlinear TD is employed to estimate the time derivative of virtual control law. As a result, the complexity of control law can be reduced without resorting to the dynamic surface control [13], [31]–[33].

Remark 3: Compared with the path following designs in [7], [46], [48], and [49] where there exist one path and one follower, multiple vehicles are required to follow one path herein. This means that a team of ASVs can be guided by one path.

IV. Stability Analysis

The closed-loop system consisting of the observer error dynamics and distributed formation maneuvering error dynamics can be expressed by

$$\Sigma_1 : \dot{E}_i = A_{0i} E_{io} + r_i S_{Ti} E_{io} - B_i \dot{\zeta}_i \tag{33}$$

$$\Sigma_2 : \begin{cases} \dot{z}_{1i} = -r_i S z_{1i} - \frac{K_{1i} q_i}{\sqrt{\|q_i\|^2 + \Delta_{1i}^2}} + a_{si}(-\tilde{\nu}_i + z_{2i}) \\ \qquad + a_{i0} R_i^T \eta_0^\theta(\theta) \vartheta + \sum_{j=1}^N a_{ij} R_i^T R_j \tilde{\nu}_j \\ \dot{z}_{2i} = -\frac{K_{2i} z_{2i}}{\sqrt{\|z_{2i}\|^2 + \Delta_{2i}^2}} + \tilde{\nu}_{id}^c - K_{2i}^o R_i^T \tilde{\eta}_i \\ \qquad - a_{si} q_i. \end{cases} \tag{34}$$

The stability of subsystem Σ_1 in (33) can be described as follows.

Lemma 1: If Assumption 1 is satisfied, the error dynamics in (33) with the state vector being E_{io} and the input vector being $\dot{\zeta}_i$ is input-to-state stable, and the estimation errors are bounded by

$$\|E_{io}(t)\| \le \sqrt{\frac{\lambda_{\max}(P_i)}{\lambda_{\min}(P_i)}} \max \left\{ \|E_{io}(t_0)\| e^{-\gamma_{1i}(t-t_0)}, \frac{2\|P_i B_i\| \zeta_i^*}{\varrho_i \bar{\theta}_i} \right\}, \ \forall t \ge t_0 \tag{35}$$

and

$$\|X_i(t)\| \le \sqrt{\frac{\lambda_{\max}(P_i)}{\lambda_{\min}(P_i)}} \max \left\{ \|X_i(t_0)\| e_i^{-\gamma_{1i}(t-t_0)}, \frac{2\|P_i B_i\| \zeta_i^*}{\varrho_i \bar{\theta}_i} \right\}, \ \forall t \ge t_0 \tag{36}$$

where $\gamma_{1i} = ([\varrho_i(1-\bar{\theta}_i)]/[\lambda_{\max}(P_i)])$ and $0 < \bar{\theta}_i < 1$ provided that

$$\begin{cases} A_{0i}^T P_i + P_i A_{0i} + \varrho_i I \le \bar{r}_i^* \left(S_{Ti}^T P_i + P_i S_{Ti} \right) \\ A_{0i}^T P_i + P_i A_{0i} + \varrho_i I \le -\bar{r}_i^* \left(S_{Ti}^T P_i + P_i S_{Ti} \right) \end{cases} \tag{37}$$

where $\bar{r}_i^* \in \Re$ is a bound satisfying $|r_i| \le \bar{r}_i^*$ and $\varrho_i \in \Re$ is a positive constant.

Proof: Construct a function $V_i = (1/2) E_{io}^T P_i E_{io}$ and its time derivative is given by

$$\dot{V}_i = \frac{1}{2} E_{io}^T \left[P_i A_{0i} + A_{0i}^T P_i + r_i \left(P_i S_{Ti} + S_{Ti}^T P_i \right) \right] E_{io} - E_{io}^T P_i B_i \dot{\zeta}_i. \tag{38}$$

Using (37), it follows that $\dot{V}_i \le -(\varrho_i/2)\|E_{io}\|^2 + \|E_{io}\| \|P_i B_i\| \|\dot{\zeta}_i\|$.

As $\|E_{io}\| \ge [(2\|P_i B_i\| \|\dot{\zeta}_i\|)/(\varrho_i \bar{\theta}_i)]$ renders

$$\dot{V}_i \le -\frac{\varrho_i}{2}(1 - \bar{\theta}_i) \|E_{io}\|^2 \tag{39}$$

it follows that subsystem (20) is ISS. Note that V_i bounded by $([\lambda_{\min}(P_i)]/2)\|E_{io}\|^2 \le V_i \le ([\lambda_{\max}(P_i)]/2)\|E_{io}\|^2$. $\|E_{io}(t)\|$ is bounded as (35). Noting that $\|E_{io}\| = \|\tilde{X}_i\|$, it leads to (36). ∎

The stability of subsystem Σ_2 in (34) is stated as below.

Lemma 2: The subsystem Σ_2 in (34) is input-to-state stable outside the connectivity preservation and collision avoidance range.

Proof: Consider a Lyapunov function candidate as

$$V_c = \frac{1}{2} \sum_{i=1}^N \left(z_{1i}^T z_{1i} + z_{2i}^T z_{2i} + a_{si} \sum_{j=1}^N \left(V_{ij}^c + V_{ij}^m \right) + 2 a_{si} \sum_{k=1}^{N_o} V_{ik}^o \right) + \frac{\vartheta^2}{2\lambda\mu}. \tag{40}$$

Taking the time derivative of V_c and using (34), it follows that:

$$\dot{V}_c = \sum_{i=1}^N \left(-q_i^T K_{1i}' q_i + q_i^T \sum_{j=1}^N a_{ij} R_i^T R_j \tilde{\nu}_j - z_{2i}^T K_{2i}' z_{2i} + z_{2i}^T \tilde{\nu}_{id}^c - z_{2i}^T K_{2i}^o R_i^T \tilde{\eta}_i + z_{3i}^T \bar{\nu}_i \right) - \frac{\vartheta^2}{\mu} \tag{41}$$

where $\bar{\nu}_i = \sum_{j=0}^N a_{ij} \dot{\eta}_j - \sum_{j=0}^N a_{ij} \dot{\eta}_{ijd}$, $K_{1i}' = K_{1i}/\sqrt{\|q_i\|^2 + \Delta_{1i}^2}$, and $K_{2i}' = K_{2i}/\sqrt{\|z_{2i}\|^2 + \Delta_{2i}^2}$. Then, one has

$$\dot{V}_c \le \sum_{i=1}^N \left(-\lambda_{\min}(K_{1i}') \|q_i\|^2 - \lambda_{\min}(K_{2i}') \|z_{2i}\|^2 + \|q_i\| \sum_{j=1}^N a_{ij} \|\tilde{\nu}_j\| + \|z_{2i}\| \|\tilde{\nu}_{id}^c\| + \lambda_{\max}(K_{2i}^o) \|z_{2i}^T\| \|\tilde{\eta}_i\| + \|z_{3i}\| \|\bar{\nu}_i\| \right) - \frac{\vartheta^2}{\mu}. \tag{42}$$

Define $q = [q_1^T, \ldots, q_N^T]^T$, $z_1 = [z_{11}^T, \ldots, z_{1N}^T]^T$, $z_2 = [z_{21}^T, \ldots, z_{2N}^T]^T$, $E_1 = [z_1^T, z_2^T, \vartheta]^T$, and $\varrho_c = \min_{i=1,\ldots,N}(\lambda_{\min}(K_{1i}'), \lambda_{\min}(K_{2i}'), 1/\mu)$.

Outside the connectivity preservation and collision avoidance range $\bar{R} < \|p_{ij}\| < \bar{R}_m$, $(\partial V_{ij}^c/\partial \eta_i) = 0$, and $(\partial V_{ij}^m/\partial \eta_i) = 0$. Hence, $q_i = z_{1i}$ and we have

$$\dot{V}_c \le -\varrho_c \|E_1\|^2 + \|E_1\| \sum_{i=1}^{N} \left(a_{si}^* \|\tilde{\nu}_i\| + \lambda_{\max}\left(K_{2i}^o\right)\|\tilde{\eta}_i\| + \left\|\tilde{\nu}_{id}^c\right\|\right) \tag{43}$$

and

$$\dot{V}_c \le -\varrho_c\left(1-\bar{\theta}\right)\|E_1\|^2 - \left(\bar{\theta}\varrho_c\|E_1\|^2 - \|E_1\| \sum_{i=1}^{N}\left(\hbar_i\|E_{io}\| + \left\|\tilde{\nu}_{id}^c\right\|\right)\right)$$

where $a_{si}^* = \sum_{j=1}^{N} a_{ji}$ and $\hbar_i = \max_{i=1,\ldots,N}\{a_{si}^*,\ \lambda_{\max}(K_{2i}^o)\}$.

Noting that

$$\|E_1\| \ge \frac{\sum_{i=1}^{N}\left(\hbar_i\|E_{io}\| + \left\|\tilde{\nu}_{id}^c\right\|\right)}{\bar{\theta}\varrho_c} \tag{44}$$

renders

$$\dot{V}_c \le -\varrho_c\left(1-\bar{\theta}\right)\|E_1\|^2 \tag{45}$$

it can be concluded that subsystem (33) is ISS.

Choosing

$$\kappa_{p1}(s) = \frac{\lambda_{\min}(P_c)}{2}s^2, \kappa_{p2}(s) = \frac{\lambda_{\max}(P_c)}{2}s^2 \tag{46}$$

with $P_c = \text{diag}\{1, a_{si}, 1/\lambda\mu\}$, it follows that:

$$\|E_1(t)\| \le \sqrt{\frac{\lambda_{\max}(P_c)}{\lambda_{\min}(P_c)}} \max\left\{\|E_1(t_0)\|e^{-\gamma_{2i}(t-t_0)}, \sum_{i=1}^{N}\frac{\hbar_i\|E_{io}\| + \left\|\tilde{\nu}_{id}^c\right\|}{\varrho_c\bar{\theta}}\right\},\ \forall t \ge t_0 \tag{47}$$

where $\gamma_{2i} = ([2\varrho_c(1-\bar{\theta})]/[\lambda_{\max}(P_c)])$. ■

The stability of the closed-loop formation control system cascaded by (33) and (34) is stated as below.

Theorem 1: Consider the ASV dynamics in (7), (8) together with the nonlinear state observer (16), the control law (25), (29), and the path update law (27). If Assumptions 1 and 2 are satisfied, the distributed formation maneuvering control with collision avoidance and connectivity preservation can be achieved, and all signals in the closed-loop distributed formation maneuvering system are uniformly ultimately bounded.

Proof: The proof is divided into two parts. We first prove the stability of closed-loop system outside the collision avoidance and connectivity reservation range. By applying [20, Lemma 1] and using Lemmas 1 and 2, the closed-loop system cascaded by subsystem Σ_1 and subsystem Σ_2 is ISS. Noting that $\dot{\zeta}_i$ and $\tilde{\nu}_{id}^c$ are bounded by ζ_i^* and l_{id}^*, respectively, it follows from (47) and (35) that $\|E_1\|$ is ultimately bounded by

$$\|E_1\| \le \sqrt{\frac{\lambda_{\max}(P_c)}{\lambda_{\min}(P_c)}} \sum_{i=1}^{N}\left\{\sqrt{\frac{\lambda_{\max}(P_i)}{\lambda_{\min}(P_i)}}\frac{2h_i\|P_iB_i\|\zeta_i^*}{\varrho_i\varrho_c\bar{\theta}_i\bar{\theta}} + \frac{l_{id}^*}{\varrho_c\bar{\theta}}\right\}. \tag{48}$$

Let $e = [e_1^T, \ldots, e_N^T]^T$, where $e_i = \eta_i - \mathcal{P}_i - \eta_0$, and then $z_1 = (H \otimes I_3)e$, where $H = D - A$ with $D = \text{diag}\{d_i\} \in \Re^{N\times N}$ and $A = [a_{ij}] \in \Re^{N\times N}$. Under Assumption 1, H is nonsingular, and we obtain $\|e\| \le \|z_1\|/\underline{o}(H)$, where $\underline{o}(H)$ is the smallest singular value of H. Hence,

$$\|e\| \le \frac{1}{\underline{o}(H)}\sqrt{\frac{\lambda_{\max}(P_c)}{\lambda_{\min}(P_c)}} \sum_{i=1}^{N}\left\{\sqrt{\frac{\lambda_{\max}(P_i)}{\lambda_{\min}(P_i)}}\frac{2h_i\|P_iB_i\|\zeta_i^*}{\varrho_i\varrho_c\bar{\theta}_i\bar{\theta}} + \frac{l_{id}^*}{\varrho_c\bar{\theta}}\right\} \tag{49}$$

implying (11). Since ϑ is bounded, there exists l_2 such that (12) is satisfied. This means that control objectives (11) and (12) are achieved.

Next, we prove the stability of the distributed formation control system where the ASVs are inside the collision avoidance and connectivity preservation range, that is, $\underline{R} < \|p_{ij}\| \le \bar{R}$ and $\underline{R}_m \le \|p_{ij}\| < \bar{R}_m$. Recalling (41), it follows that:

$$\dot{V}_c \le \sum_{i=1}^{N}\left(-q_i^TK_{1i}'q_i + q_i^T\sum_{j=1}^{N}a_{ij}R_i^TR_j\tilde{\nu}_j - z_{2i}^TK_{2i}'z_{2i} + z_{2i}^T\tilde{\nu}_{id}^c - z_{2i}^TK_{2i}^oR_i^T\tilde{\eta}_i + a_{si}z_{3i}^T\bar{\nu}_i\right) - \frac{\vartheta^2}{\mu} \tag{50}$$

and

$$\dot{V}_c \le \sum_{i=1}^{N}\left(-\lambda_{\min}\left(K_{1i}'\right)\|q_i\|^2 - \lambda_{\min}\left(K_{2i}'\right)\|z_{2i}\|^2 + \|q_i\|\sum_{j=1}^{N}a_{ij}\left\|\tilde{\nu}_j\right\| + \|z_{2i}\|\left\|\tilde{\nu}_{id}^c\right\| + \lambda_{\max}\left(K_{2i}^o\right)\|z_{2i}\|\|\tilde{\eta}_i\|\right) - \frac{\vartheta^2}{\mu}. \tag{51}$$

Letting $E_2 = [q^T, z_2^T, \vartheta]^T$, it follows that:

$$\dot{V}_c \le -\varrho_c\left(1-\bar{\theta}\right)\|E_2\|^2 - \left(\bar{\theta}\varrho_c\|E_2\|^2 - \|E_2\|\sum_{i=1}^{N}\left(\hbar_i\|E_{io}\| + \left\|\tilde{\nu}_{id}^c\right\|\right)\right).$$

Noting that

$$\|E_2\| \ge \frac{\sum_{i=1}^{N}\left(\hbar_i\|E_{io}\| + \left\|\tilde{\nu}_{id}^c\right\|\right)}{\bar{\theta}\varrho_2} \tag{52}$$

renders

$$\dot{V}_c \le -\varrho_c\left(1-\bar{\theta}\right)\|E_2\|^2. \tag{53}$$

Since E_{io} and $\tilde{\nu}_{id}^c$ are bounded, it follows that all signals in E_2 are bounded and V_c is nonincreasing when the ASVs are inside the collision avoidance and connectivity preservation range. Since $V_{ij}^c = \infty$ as $\|p_{ij}\| = \underline{R}$, $V_{ij}^o = \infty$ as $\|p_{ij}\| = \underline{R}_o$, and $V_{ij}^m = \infty$ as $\|p_{ij}\| = \underline{R}_m$, there is no collisions between ASVs, static obstacles can be avoided, and connectivity is maintained if the vehicle networks are initially connected. As a result, the control objectives (13) and (14) are achieved. ■

Since the proposed observer is stable in terms of uniform ultimate boundedness, asymptotically stable of the closed-loop system could not be derived in the presented work.

Remark 4: A parameter selection guide is provided as follows. The parameter ω_i is selected by considering sampling

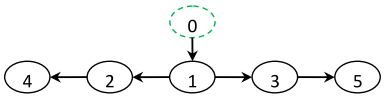

Fig. 2. Communication graph in the simulation.

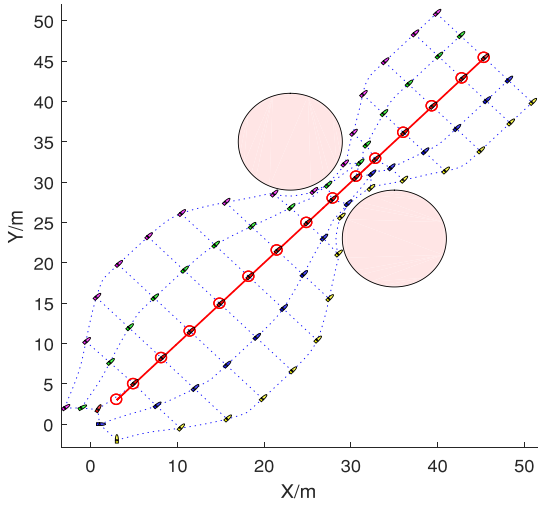

Fig. 3. Time-varying formation pattern with collision avoidance and connectivity preservation.

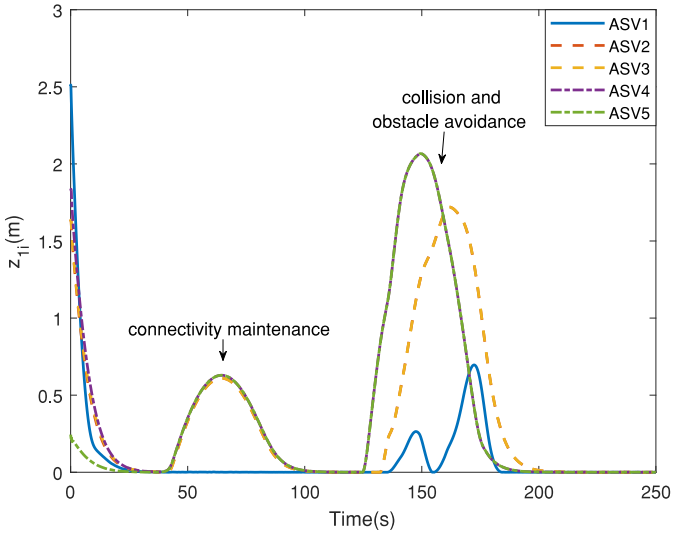

Fig. 4. Cooperative time-varying formation maneuvering errors.

rate and measurement noises. K_{1i} and K_{2i} are chosen based on the maximal velocity and control input. Δ_{1i} and Δ_{2i} are selected according to the desired transient performance. a_{si} is chosen according to the communication graph.

V. Simulation Results

A coordinated formation control system consisting of five ships is considered to illustrate the control performance of the proposed distributed time-varying formation maneuvering control laws. The surface vehicle employed in the simulation is Cybership II developed at Norwegian University of Science and Technology and its parameters are given in [46]. The virtual leader is set to move along a path parameterized by

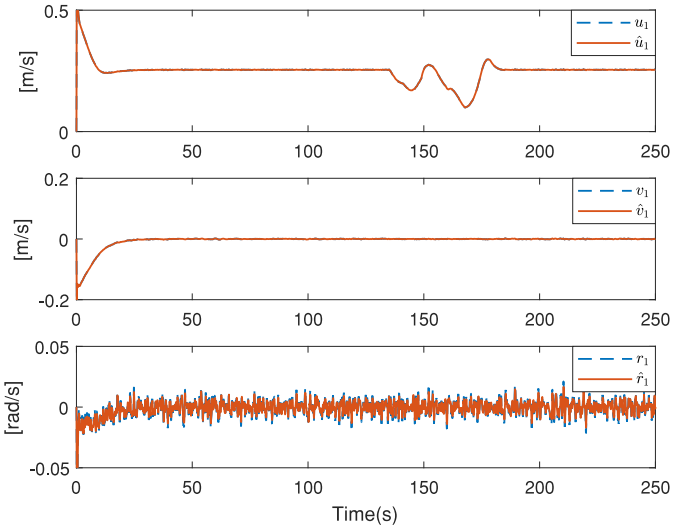

Fig. 5. Velocity recovery performance using the proposed state observer.

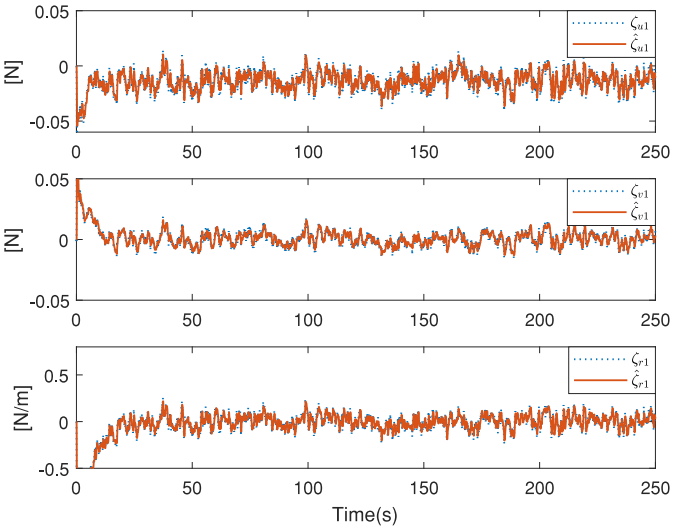

Fig. 6. Disturbance estimation using the proposed state observer.

$\eta_0(\theta) = [0.09\theta + 3, 0.09\theta + 3, \pi/4]^T$. The communication graph among the five vehicles is given in Fig. 2 and a time-varying formation pattern is set to $\eta_{1d} = [0, 0, 0]^T$, $\eta_{2d} = [-a, -a, 0]^T$, $\eta_{3d} = [a, -a, 0]^T$, $\eta_{4d} = [-2a, 2a, 0]^T$, and $\eta_{5d} = [2a, -2a, 0]^T$, where $a = 2.8 - 1.8\cos((t + 30)/30)$, $t < 200$; $a = 2.76 - 0.003(t - 210)^2$, $200 < t < 210$; and $a = 2.76$, $t > 210$.

The parameters for the proposed control laws are set to $K_{1i} = \text{diag}\{0.2, 0.2, 0.2\}$, $\Delta_{1i} = 1$, $\Delta_{2i} = 1$, $K_{2i} = \text{diag}\{129, 169, 13.8\}$, $\omega_i = 20$, $\gamma_i = 10$, $\lambda = 10$, and $\mu = 10$. The parameters for the potential functions are selected as $\underline{R} = 1$, $\bar{R} = 2$, $\underline{R}_m = 5$, $\bar{R}_m = 6$, $\underline{R}_o = 6$, and $\bar{R}_o = 7$. The positions of two static obstacles are set as $[23, 35]^T$ and $[35, 23]^T$ with a radius 6. Simulation results on the proposed output-feedback control method for time-varying formation maneuvering are illustrated in Figs. 3–8. Fig. 3 shows the time-varying formation pattern shaped by the five vehicles, which is guided by a virtual leader moving along the parameterized path. It can be observed that collisions between vehicles

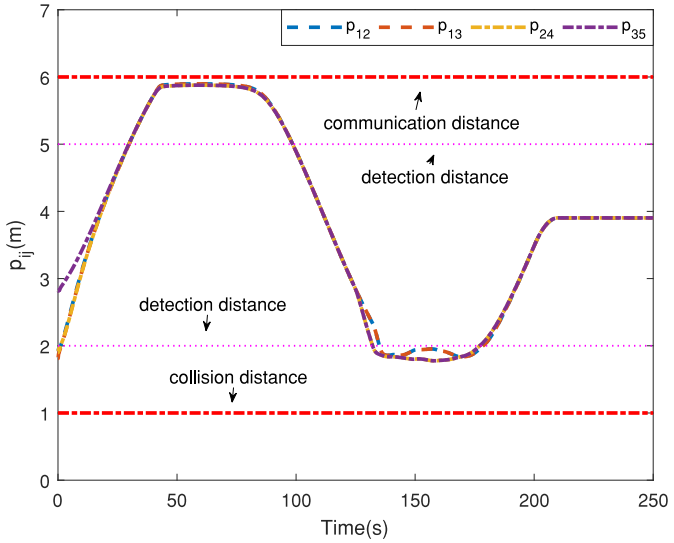

Fig. 7. Collision avoidance and connectivity preservation performance.

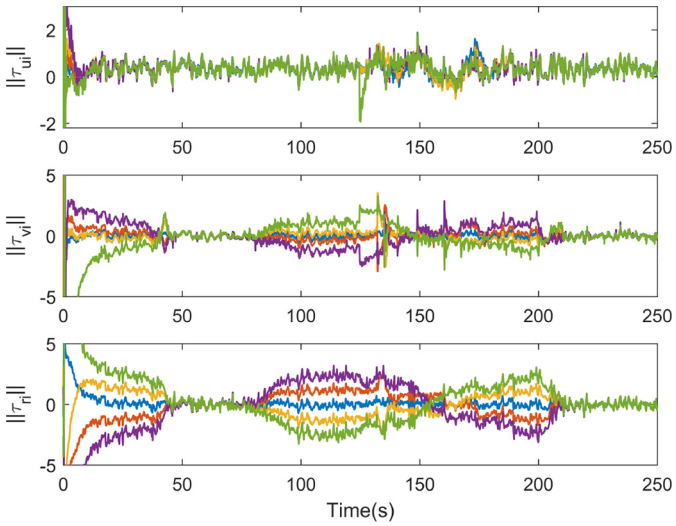

Fig. 8. Control inputs of torque and moment.

and obstacles are avoided. Fig. 4 depicts the cooperative time-varying formation maneuvering errors of the five ships. During 0–45 s, the cooperative time-varying formation errors approach zero regardless of unknown internal and external disturbances as well as unmeasured velocity information. During 45–100 s, the connectivity preservation take a higher priority than the distributed formation maneuvering task, leading to large time-varying formation maneuvering errors. However, the time-varying formation maneuvering errors converge to a small neighborhood of the origin when the desired formation pattern is within the connectivity maintenance range. During 100–200 s, the five vehicles try to avoid the obstacles in a cooperative fashion. During 200–250 s, a static line formation pattern is stabilized with small tracking errors. Fig. 5 demonstrates that the state recovery performance of the proposed state observer, and it implies the surge, sway, and yaw rate can be accurately reconstructed by using the output information of position and yaw heading. Fig. 6 shows that the internal uncertainties and external disturbances can be estimated by the proposed nonlinear observer. Fig. 7 depicts the control performance of connectivity maintenance and collision avoidance. It shows that relative range are within the connectivity maintenance range without violating the collision avoidance constraints. Fig. 8 depicts the control force and moment of each ship and the control signals are bounded.

Discussion: In the proposed control design, the distributed time-varying formation maneuvering laws are proposed for fully actuated vehicles. To address the distributed time-varying formation maneuvering of under-actuated vehicles, several methods may be applied, such as the transverse function approach, coordinate transformation, and auxiliary variable method. This deserves to investigate in future works.

VI. Conclusion

This paper investigated the cooperative time-varying formation maneuvering with connectivity preservation and collision avoidance for multiple ASVs in the presence of position–heading measurements only. Each vehicle is subject to unknown kinetics induced by internal model uncertainty and external disturbances caused by wind, waves, and ocean currents. At first, a nonlinear state observer is developed for recovering the unmeasured velocity and yaw rate as well as unknown uncertainty and disturbances. Then, distributed output feedback time-varying formation maneuvering control laws are designed based on the backstepping technique, nonlinear tracking differentiators, and artificial potential functions. The stability of closed-loop distributed formation control system is analyzed based on input-to-state stability and cascade stability. Simulation results substantiate the proposed output feedback method for cooperative time-varying formation maneuvering of ASVs with capabilities of connectivity preservation and collision avoidance. For future works, it is rewarding to investigate the distributed formation maneuvering of under-actuated ASVs with connectivity preservation and collision avoidance.

References

[1] Y. Shi, C. Shen, H. Fang, and H. Li, "Advanced control in marine mechatronic systems: A survey," *IEEE/ASME Trans. Mechatronics*, vol. 22, no. 3, pp. 1121–1131, Jun. 2017.

[2] X. Xiang, C. Yu, L. Lapierre, J. Zhang, and Q. Zhang, "Survey on fuzzy-logic-based guidance and control of marine surface vehicles and underwater vehicles," *Int. J. Fuzzy Syst.*, vol. 20, no. 2, pp. 572–586, 2018.

[3] Z. Yan and J. Wang, "Model predictive control for tracking of under-actuated vessels based on recurrent neural networks," *IEEE J. Ocean. Eng.*, vol. 37, no. 4, pp. 717–726, Oct. 2012.

[4] Z. Zheng, Y. Huang, L. Xie, and B. Zhu, "Adaptive trajectory tracking control of a fully actuated surface vessel with asymmetrically constrained input and output," *IEEE Trans. Control Syst. Technol.*, vol. 26, no. 5, pp. 1851–1859, Sep. 2018.

[5] Z. Peng, J. Wang, and J. Wang, "Constrained control of autonomous underwater vehicles based on command optimization and disturbance estimation," *IEEE Trans. Ind. Electron.*, vol. 66, no. 5, pp. 3627–3635, May 2019.

[6] B. Miao, T. Li, and W. Luo, "A DSC and MLP based robust adaptive NN tracking control for underwater vehicle," *Neurocomputing*, vol. 111, pp. 184–189, Jul. 2013.

[7] Z. Peng, J. Wang, and Q.-L. Han, "Path-following control of autonomous underwater vehicles subject to velocity and input constraints via neurodynamic optimization," *IEEE Trans. Ind. Electron.*, to be published.

[8] H. Li, P. Xie, and W. Yan, "Receding horizon formation tracking control of constrained underactuated autonomous underwater vehicles," *IEEE Trans. Ind. Electron.*, vol. 64, no. 6, pp. 5004–5013, Jun. 2017.

[9] H. Li and W. Yan, "Model predictive stabilization of constrained underactuated autonomous underwater vehicles with guaranteed feasibility and stability," *IEEE/ASME Trans. Mechatronics*, vol. 22, no. 3, pp. 1185–1194, Jun. 2017.

[10] R. Cui, W. Yan, and D. Xu, "Synchronization of multiple autonomous underwater vehicles without velocity measurements," *Sci. China Inf. Sci.*, vol. 55, no. 7, pp. 1693–1703, Jul. 2012.

[11] M. Chen, B. Jiang, and R. Cui, "Actuator fault-tolerant control of ocean surface vessels with input saturation," *Int. J. Robust Nonlin. Control*, vol. 26, no. 3, pp. 542–564, Feb. 2015.

[12] R. Cui, S. S. Ge, B. V. E. How, and Y. S. Choo, "Leader–follower formation control of underactuated autonomous underwater vehicles," *Ocean Eng.*, vol. 37, nos. 17–18, pp. 1491–1502, Dec. 2010.

[13] Z. Peng, D. Wang, Z. Chen, X. Hu, and W. Lan, "Adaptive dynamic surface control for formations of autonomous surface vehicles with uncertain dynamics," *IEEE Trans. Control Syst. Technol.*, vol. 21, no. 2, pp. 513–520, Mar. 2013.

[14] X. Jin, "Fault tolerant finite-time leader–follower formation control for autonomous surface vessels with LOS range and angle constraints," *Automatica*, vol. 68, pp. 228–236, Jun. 2016.

[15] S. Li and X. Wang, "Finite-time consensus and collision avoidance control algorithms for multiple AUVs," *Automatica*, vol. 49, no. 11, pp. 3359–3367, Nov. 2013.

[16] Z. Peng, J. Wang, and D. Wang, "Containment maneuvering of marine surface vehicles with multiple parameterized paths via spatial–temporal decoupling," *IEEE/ASME Trans. Mechatronics*, vol. 22, no. 2, pp. 1026–1036, Apr. 2017.

[17] Z. Peng, J. Wang, and D. Wang, "Distributed containment maneuvering of multiple marine vessels via neurodynamics-based output feedback," *IEEE Trans. Ind. Electron.*, vol. 64, no. 5, pp. 3831–3839, May 2017.

[18] Z. Peng, J. Wang, and D. Wang, "Distributed maneuvering of autonomous surface vehicles based on neurodynamic optimization and fuzzy approximation," *IEEE Trans. Control Syst. Technol.*, vol. 26, no. 3, pp. 1083–1090, May 2018.

[19] Y. Zhang, D. Wang, and Z. Peng, "Consensus maneuvering for a class of nonlinear multivehicle systems in strict-feedback form," *IEEE Trans. Cybern.*, vol. 49, no. 5, pp. 1759–1767, May 2019.

[20] Z. Peng, D. Wang, and J. Wang, "Cooperative dynamic positioning of multiple marine offshore vessels: A modular design," *IEEE/ASME Trans. Mechatronics*, vol. 21, no. 3, pp. 1210–1221, Jun. 2015.

[21] M. Fu and L. Yu, "Finite-time extended state observer-based distributed formation control for marine surface vehicles with input saturation and disturbances," *Ocean Eng.*, vol. 159, pp. 219–227, Jul. 2018.

[22] J. A. Fax and R. M. Murray, "Information flow and cooperative control of vehicle formations," *IEEE Trans. Autom. Control*, vol. 49, no. 9, pp. 1465–1476, Sep. 2004.

[23] Z. Peng, D. Wang, H. Zhang, and G. Sun, "Distributed neural network control for adaptive synchronization of uncertain dynamical multiagent systems," *IEEE Trans. Neural Netw. Learn. Syst.*, vol. 25, no. 8, pp. 1508–1519, Aug. 2014.

[24] H. Li, Y. Shi, and W. Yan, "Distributed receding horizon control of constrained nonlinear vehicle formations with guaranteed γ-gain stability," *Automatica*, vol. 68, pp. 148–154, Jun. 2016.

[25] D. Wang, N. Zhang, J. Wang, and W. Wang, "Cooperative containment control of multiagent systems based on follower observers with time delay," *IEEE Trans. Syst., Man, Cybern., Syst.*, vol. 47, no. 1, pp. 13–23, Jun. 2017.

[26] Z. Peng, D. Wang, Y. Shi, H. Wang, and W. Wang, "Containment control of networked autonomous underwater vehicles with model uncertainty and ocean disturbances guided by multiple leaders," *Inf. Sci.*, vol. 316, no. 12, pp. 163–179, Sep. 2015.

[27] L. Cheng, Y. Wang, W. Ren, Z.-G. Hou, and M. Tan, "Containment control of multiagent systems with dynamic leaders based on a PI^n-type approach," *IEEE Trans. Cybern.*, vol. 46, no. 12, pp. 3004–3017, Dec. 2016.

[28] H. Liu, L. Cheng, M. Tan, and Z.-G. Hou, "Containment control of continuous-time linear multi-agent systems with aperiodic sampling," *Automatica*, vol. 57, pp. 78–84, Jul. 2015.

[29] W. Li, L. Liu, and G. Feng, "Distributed containment tracking of multiple stochastic nonlinear system," *Automatica*, vol. 69, pp. 214–221, Jul. 2016.

[30] C. Shen, Y. Shi, and B. Buckham, "Trajectory tracking control of an autonomous underwater vehicle using Lyapunov-based model predictive control," *IEEE Trans. Ind. Electron.*, vol. 65, no. 7, pp. 5796–5805, Jul. 2018.

[31] S.-L. Dai, S. He, H. Lin, and C. Wang, "Platoon formation control with prescribed performance guarantees for USVs," *IEEE Trans. Ind. Electron.*, vol. 65, no. 5, pp. 4237–4246, May 2018.

[32] S. He, M. Wang, S.-L. Dai, and F. Luo, "Leader–follower formation control of USVs with prescribed performance and collision avoidance," *IEEE Trans. Ind. Informat.*, vol. 15, no. 1, pp. 572–581, Jan. 2019.

[33] B. S. Park and S. J. Yoo, "An error transformation approach for connectivity-preserving and collision-avoiding formation tracking of networked uncertain underactuated surface vessels," *IEEE Trans. Cybern.*, vol. 49, no. 8, pp. 2955–2966, Aug. 2019.

[34] H. Su, X. Wang, and G. Chen, "Rendezvous of multiple mobile agents with preserved network connectivity," *Syst. Control Lett.*, vol. 59, no. 5, pp. 313–322, May 2010.

[35] Y. Dong and J. Huang, "Flocking with connectivity preservation of multiple double integrator systems subject to external disturbances by a distributed control law," *Automatica*, vol. 55, pp. 197–203, May 2015.

[36] Y. Dong and J. Huang, "Leader-following connectivity preservation rendezvous of multiple double integrator systems based on position measurement only," *IEEE Trans. Autom. Control*, vol. 59, no. 9, pp. 2598–2603, Sep. 2014.

[37] Y. Dong, Y. Su, Y. Liu, and S. Xu, "An internal model approach for multi-agent rendezvous and connectivity preservation with nonlinear dynamics," *Automatica*, vol. 89, pp. 300–307, Mar. 2018.

[38] Y. Su, "Leader-following rendezvous with connectivity preservation and disturbance rejection via internal model approach," *Automatica*, vol. 57, pp. 203–212, Jul. 2015.

[39] I. F. Ihle, R. Skjetne, and T. I. Fossen, "Output feedback control for maneuvering systems using observer backstepping," in *Proc. 13th Mediterr. Conf. Control Autom. Intell. Control*, 2005, pp. 1512–1517.

[40] R. Cui, L. Chen, C. Yang, and M. Chen, "Extended state observer-based integral sliding mode control for an underwater robot with unknown disturbances and uncertain nonlinearities," *IEEE Trans. Ind. Electron.*, vol. 64, no. 8, pp. 6785–6795, Aug. 2018.

[41] Y. Li and S. Tong, "Adaptive fuzzy output-feedback stabilization control for a class of switched nonstrict-feedback nonlinear systems," *IEEE Trans. Cybern.*, vol. 47, no. 4, pp. 1007–1016, Apr. 2016.

[42] Y. Li and S. Tong, "Adaptive fuzzy output constrained control design for multi-input multioutput stochastic nonstrict-feedback nonlinear systems," *IEEE Trans. Cybern.*, vol. 47, no. 12, pp. 4086–4095, Dec. 2017.

[43] L. Liu, D. Wang, and Z. Peng, "State recovery and disturbance estimation of unmanned surface vehicles based on nonlinear extended state observers," *Ocean Eng.*, vol. 171, pp. 625–632, Jan. 2019.

[44] R. Skjetne, S. Moi, and T. I. Fossen, "Nonlinear formation control of marine craft," in *Proc. 41st IEEE Conf. Decis. Control*, vol. 2. Las Vegas, NV, USA, 2002, pp. 1699–1704.

[45] S. Mastellone, D. M. Stipanović, C. R. Graunke, K. A. Intlekofer, and M. W. Spong, "Formation control and collision avoidance for multi-agent non-holonomic systems: Theory and experiments," *Int. J. Robot. Res.*, vol. 27, no. 1, pp. 107–126, Jan. 2008.

[46] R. Skjetne, T. I. Fossen, and P. V. Kokotović, "Adaptive maneuvering, with experiments, for a model ship in a marine control laboratory," *Automatica*, vol. 41, no. 2, pp. 289–298, Feb. 2005.

[47] B.-Z. Guo and Z.-L. Zhao, "Weak convergence of nonlinear high-gain tracking differentiator," *IEEE Trans. Autom. Control*, vol. 58, no. 4, pp. 1074–1080, Apr. 2013.

[48] X. Xiang, L. Lapierre, and B. Jouvencel, "Smooth transition of AUV motion control: From fully-actuated to under-actuated configuration," *Robot. Auton. Syst.*, vol. 67, pp. 14–22, May 2015.

[49] X. Xiang, C. Yu, and Q. Zhang, "Robust fuzzy 3D path following for autonomous underwater vehicle subject to uncertainties," *Comput. Oper. Res.*, vol. 84, pp. 165–177, Sep. 2017.